Journal of Histochemistry & Cytochemistry 60(7) 521–529
© The Author(s) 2012
Reprints and permission:
sagepub.com/journalsPermissions.nav
DOI: 10.1369/0022155412446227
http://jhc.sagepub.com
SAGE

Cisplatin Nephrotoxicity Involves Mitochondrial Injury with Impaired Tubular Mitochondrial Enzyme Activity

Zsuzsanna K. Zsengellér, Lena Ellezian, Dan Brown, Béla Horváth, Partha Mukhopadhyay, Balaraman Kalyanaraman, Samir M. Parikh, S. Ananth Karumanchi, Isaac E. Stillman, and Pál Pacher

Department of Pathology (ZKZ, LE, DB, IES), Renal Division, Department of Medicine (SMP, SAK, IES), and Center for Vascular Biology Research (SMP, SAK), Beth Israel Deaconess Medical Center, Boston, Massachusetts; Section on Oxidative Stress Tissue Injury, Laboratory of Physiologic Studies, National Institute on Alcohol Abuse and Alcoholism, National Institute of Health Bethesda, Maryland (BH, PM, PP); and Free Radical Research Center, Biophysics Department, Medical College of Wisconsin, Milwaukee, Wisconsin (BK)

Summary

Cisplatin is a widely used antineoplastic agent. However, its major limitation is dose-dependent nephrotoxicity whose precise mechanism is poorly understood. Recent studies have suggested that mitochondrial dysfunction in tubular epithelium contributes to cisplatin-induced nephrotoxicity. Here the authors extend those findings by describing the role of an important electron transport chain enzyme, cytochrome c oxidase (COX). Immunohistochemistry for COX I protein demonstrated that, in response to cisplatin, expression was mostly maintained in focally damaged tubular epithelium. In contrast, COX enzyme activity in proximal tubules (by light microscopy) was decreased. Ultrastructural analysis of the cortex and outer stripe of the outer medulla showed decreased mitochondrial mass, disruption of cristae, and extensive mitochondrial swelling in proximal tubular epithelium. Functional electron microscopy showed that COX enzyme activity was decreased in the remaining mitochondria in the proximal tubules but maintained in distal tubules. In summary, cisplatin-induced nephrotoxicity is associated with structural and functional damage to the mitochondria. More broadly, using functional electron microscopy to measure mitochondrial enzyme activity may generate mechanistic insights across a spectrum of renal disorders. (J Histochem Cytochem 60:521–529, 2012)

Keywords

cisplatin, nephrotoxicity, mitochondria, cytochrome c oxidase, functional electron microscopy

Cisplatin (or cis-diamminedichloroplatinum II) is a chemotherapeutic agent widely used against several types of solid tumors (Langerak and Dreisbach 2001). However, its clinical use is limited by its potent nephrotoxicity, which may result in acute renal failure (Ries and Klastersky 1986; Safirstein et al. 1986; Schrier 2002; Sahni et al. 2009). In the pathomechanism of this type of nephropathy, increased oxidative stress, DNA damage, inhibition of protein synthesis, and mitochondrial damage have been implicated and ultimately cause cell death in the tubular epithelium (Ramesh et al. 2002; Santos et al. 2007; Zhang et al. 2007; Mukhopadhyah et al. 2010a; Mukhopadhyah et al. 2010b; Mukhopadhyah et al. 2012). In this study, we aimed to explore the mechanisms of the mitochondrial injury.

Cytochrome c oxidase (COX, Complex IV) is a mitochondrial electron transport chain enzyme that resides in the mitochondrial inner membrane, and its activity is required to generate the proton motive force that drives downstream ATP synthesis. In a recent study using a murine cisplatin model, we have shown that COX enzyme activity is attenuated in focal areas of the cortical tubular epithelium (Mukhopadhyay et al. 2012). This work suggested the

Received for publication January 18, 2012; accepted March 21, 2012.

Corresponding Author:
Zsuzsanna K. Zsengellér, MD, PhD, Department of Pathology, Beth Israel Deaconess Medical Center, 330 Brookline Avenue, Boston MA 02215
E-mail: zzsengel@bidmc.harvard.edu

enzyme histochemical assay as a useful tool to characterize mitochondrial metabolic competence within the kidney. One limitation of this assay is the poor resolution of single cell in situ. Since the results suggested focal changes in tubular epithelial cells, we sought additional improvements to the enzyme function assay to enable visualization of this activity within individual cells of the nephron.

In this study, we explored the role of mitochondrial dysfunction in cisplatin-induced acute kidney injury. Immunohistochemistry and enzyme histochemistry on light microscopy and transmission electron microscopy level were utilized to assess structural and functional alterations in mitochondria after cisplatin treatment in mice.

Materials and Methods

Animals and Drug Treatment

All animal experiments conformed to National Institutes of Health guidelines and were approved by the Institutional Animal Care and Use Committee of the National Institute on Alcohol Abuse and Alcoholism (Bethesda, Maryland). Six- to eight-week-old male C57Bl/6J mice were obtained from the Jackson Laboratory (Bar Harbor, Maine). All animals were kept in a temperature-controlled environment with a 12-hr light-dark cycle, were allowed free access to food and water at all times, and were cared for in accordance with National Institutes of Health guidelines. Mice were sacrificed 72 hr following a single injection of cisplatin (cis-Diammineplatinum(II) dichloride, 25 mg/kg i.p.; Sigma, St. Louis, MO).

Immunohistochemistry for COX 1

Paraffin sections (5 μm) on polysine-coated slides (Fisher, Atlanta, Georgia) were deparaffinized and rehydrated. Optimal staining was achieved with an antigen retrieval method that was performed in 10 mmol/l citric acid, pH 6.00, for 15 min. Endogenous peroxidase was quenched with 3% H_2O_2 in ddH_2O for 15 min. Avidin-biotin blocking step was incorporated to eliminate nonspecific binding to endogenous avidin/biotin in kidney tissue. Sections were blocked with 2.5% normal horse serum at room temperature for 40 min and incubated 40 min with 1:500 dilution of primary COX 1 antibody (cytochrome c oxidase subunit I, or oxidative phosphorylation complex IV, subunit I) (Santa Cruz Biotechnology, Inc., Santa Cruz CA). Specific labeling was detected with a Vector MOM peroxidase kit (Vector MOM Kit, Vector Laboratories). The enzymatic reaction product was achieved by using Nova-Red substrate to give a red precipitate, and the sections were counterstained with hematoxylin, dehydrated, and mounted in Permount. Sections with no primary antibody were used as negative control slides.

In Situ Enzyme Chemistry

Light microscopy. After removal, kidneys were bivalved and frozen immediately in isopentane cooled with liquid nitrogen. The tissues were cryosectioned (6 μm thick) and stained for NADH and COX activities, as described previously (Hershey et al. 1975; Dubowitz, 1985; Lebrecht et al. 2004).

Electron microscopy. After rapid removal, kidneys were cut in both sagittal and horizontal cross sections and frozen immediately. The tissues were cryosectioned at 60 μm and fixed in 2.5% glutaraldehyde in 0.1 M Na-Cacodylate buffer (Tousimis Research Corp., Rockville, Maryland) for 30 min. Sections were washed in 0.05M PBS (pH 7.4) for 1.5 hr. The sections were treated for enzyme chemistry as described previously (Seligman et al. 1968; Anderson et al. 1975; Hershey et al. 1975; Bertoni-Freddari et al. 2001), then processed for EPON embedding by standard protocols. Sections were examined with JEOL 1011 Transmission Electron Microscope, with a Hamamatsu Orca-HR Digital Camera, and AMT (Advanced Microscopy Techniques Corp.) image capture system.

Morphometric Quantification by Electron Microscopy

Measurements were generated from transmission electron microscopy images with a magnification of ×10,000. Representative digital images of proximal tubular epithelium (cortical labyrinth) were acquired (positioned to minimize nucleus or brush border within the image). Morphometric measurements were performed in two stages using Image J software. First, to determine mitochondrial volume, non-cytoplasmic area was manually excluded from analysis. The optical density threshold was manually set to include all mitochondria, and then the percentage area of mitochondria was calculated per cytoplasmic volume. In the second stage, for measurements of COX activity per mitochondrial area, the identical JPEG images were used, but the threshold was manually set to include the COX enzyme histochemical product alone, and the mean optical density of the reaction product was calculated.

Isolation of Mitochondria From Kidneys and Determination of Nitrotyrosine and 4-Hydroxynonenal Content

Mitochondria were isolated from the kidneys of mice treated with vehicle or cisplatin using a tissue mitochondrial isolation kit (Pierce Biotechnology, Rockford, Illinois). Mitochondrial nitrotyrosine and 4-hydroxynonenal content were determined by commercially available kits, as described (Mukhopadhyay et al. 2012).

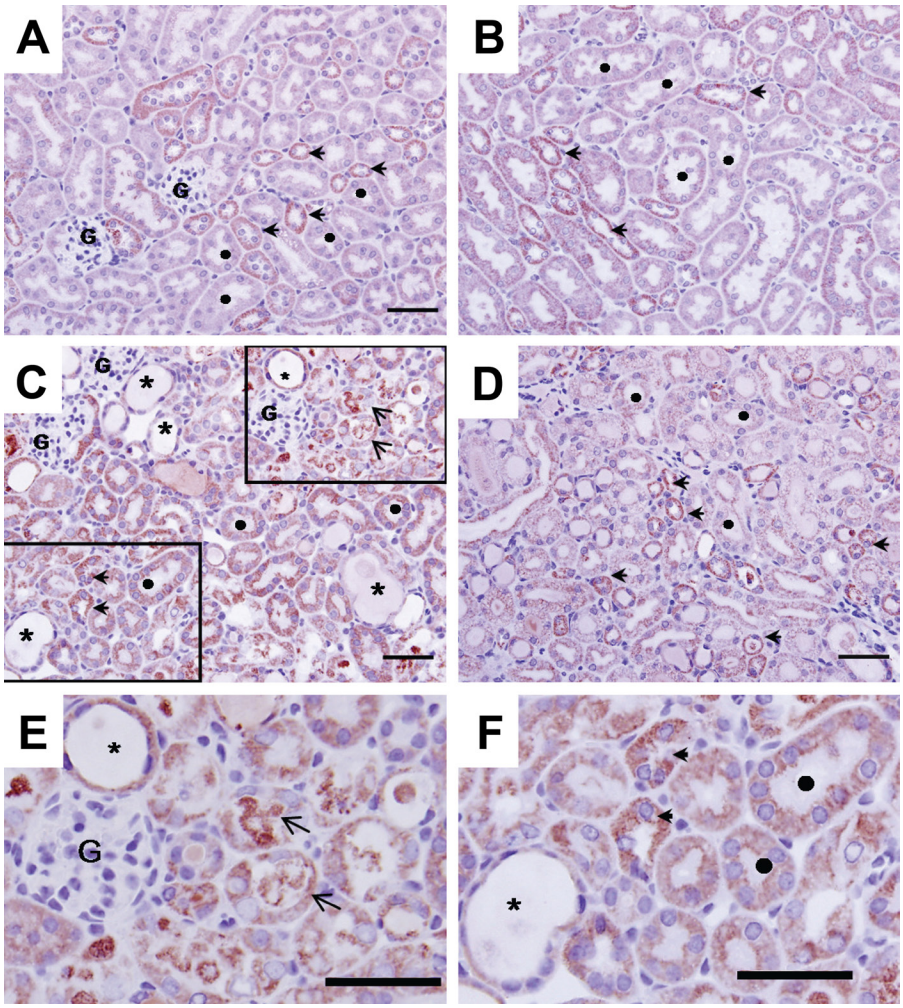

Figure 1. COX I immunohistochemistry in mouse kidney 72 hr after cisplatin treatment. Panels A and B: control sham-treated mouse kidney. Extensive immunostaining (red stain) is observed in both proximal and distal tubular epithelium; staining is mainly in the basolateral surface of the epithelia. In the cortex (Panel A), distal tubules (arrowheads) are more extensively stained for COX I than are proximal epithelium (denoted by ●). In the medulla (Panel B), distal tubules (arrowheads) also exhibit more intense staining than S3 segments of proximal tubules. Panels C, D, E, and F: Cisplatin induced profound histopathological renal injury, desquamation of epithelial cells evidenced by protein cast in the tubular lumen (arrows), and dilation of the tubules (denoted by *). COX I expression was mildly decreased in damaged tubular epithelial cells (Panel E), but immunostaining is maintained at a relatively normal distribution in spared epithelium (Panel F). Bars: A, B, C, D: 50 µm.

Statistics

Quantitative results were expressed as means ± SEM. Statistics were performed with unpaired two-tailed *t*-test. Mean differences were considered significant at $p \leq 0.05$ as indicated in the Results sections and figures.

Results

Oxidative/Nitrative Stress Markers

Reactive oxygen species play a key role in the pathomechanism of cisplatin-induced kidney injury (Pan et al. 2009; Mukhopadhyay et al. 2011; Mukhopadhyay et al. 2012). In renal mitochondrial extract from cisplatin-treated mice, we observed markedly increased 4-hydroxynonenal compared to control vehicle–injected animals (control: 100 ± 3%, n=6; cisplatin: 442 ± 74%, n=5, at 72 hr, p<0.01). Also nitrotyrosine content was increased in the mitochondrial extract in the kidney after cisplatin treatment (control: 100 ± 9%, n=6; cisplatin 72 hr: 431 ± 46%, n=8, p<0.01).

COX Immunohistochemistry

COX 1 protein expression was assessed by immunohistochemistry in kidneys of sham- and cisplatin-treated mice (Fig. 1). In control mice (Panels A and B), kidney COX expression was higher in distal than proximal tubules. Seventy-two hours after cisplatin treatment, necrotic debris was sloughed into the tubular lumen in cortex and the outer stripe of the outer medulla (OSOM; indicated by arrows in Panels C and E). Desquamation of necrotic epithelial cells resulted in patches of denuded basement membrane and dilation of proximal tubules (Panels C, E, and F; denoted by *). Focal loss of brush border in proximal tubules was also visible. COX 1 protein expression was mildly decreased in damaged tubular epithelial cells (Panel E). In contrast, COX1 expression was preserved in areas of the cortex and outer medulla that showed no light microscopic evidence of cellular injury (Panel F). The degree of proximal tubular damage (in the cortex and in OSOM) was focal and variable. COX immunostaining was preserved in mildly injured tubules (Panel F). Tubules with severe damage showed decreased but still detectable staining (Panel E).

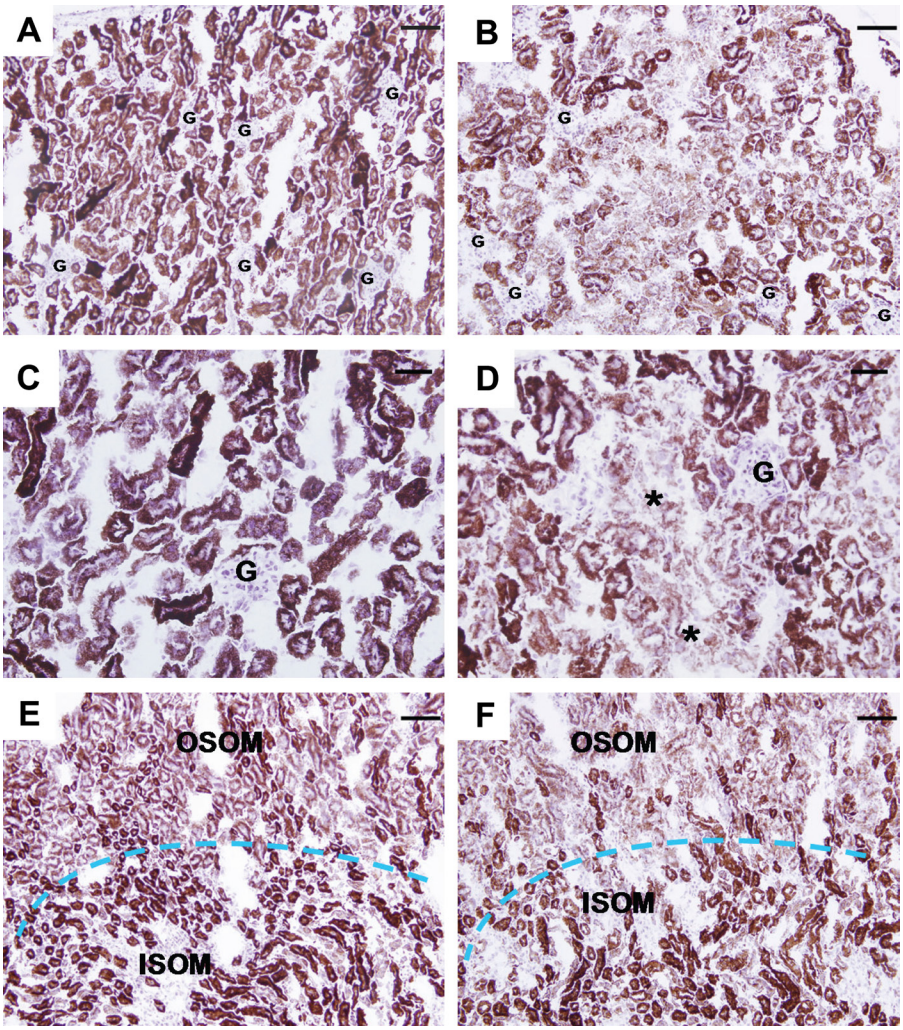

Figure 2. COX enzyme histochemistry in mouse kidney 72 hr after cisplatin treatment. Panels A and C (cortex) and E (medulla): Staining (brown) for cytochrome c oxidase enzyme activity on sections of snap-frozen kidney from sham-treated mice. The cortex (A) and inner stripe of the outer medulla (ISOM) have the most intense staining, followed by the outer stripe of the outer medulla (OSOM), with the weakest activity in the inner medulla. Panels B and D (cortex) and F (medulla): Enzyme activity in the cortex and OSOM is greatly decreased 72 hr after cisplatin treatment but unchanged in the ISOM. G: glomerulus. Bars: A, B, E, and F: 80 μm; C and D: 40 μm.

COX Enzyme Histochemistry

The activity of COX isoforms was measured using enzyme histochemistry in kidneys of sham- and cisplatin-treated mice (Fig. 2). This assay showed decreased COX enzymatic activity in the cortex and OSOM of the kidneys 72 hr after cisplatin treatment (Panels B and D, cortex; Panel F, medulla) compared to sham-treated control (Panels A and C, cortex; Panel E, medulla). This decrease in enzymatic activity after cisplatin treatment appeared more pronounced than the decrease in the expression of the COX protein. There was no difference in COX activity between the inner stripe of the outer medulla of the cisplatin-treated and control mice (Panels E and F), again emphasizing that cisplatin treatment in mice predominantly affects the cortex and OSOM of the kidneys.

Ultrastructural Analysis of COX Enzyme Activity

To visualize changes in COX enzymatic activity along the nephron more closely, we redeveloped a technique that combined transmission electron microscopy with enzyme histochemistry in kidneys of sham- and cisplatin-treated mice (Fig. 3) (Seligman et al. 1968; Anderson et al. 1975; Hershey et al. 1975; Bertoni-Freddari et al. 2001; Mahad et al. 2009). Panels A and B show strong COX activity in the mitochondria of normal kidney proximal tubules. However, 72 hr after cisplatin treatment, there was substantial damage to this organelle, including disorganization, mitochondrial swelling, disrupted cristae, and significantly decreased COX activity (Panels C and D).

Morphometric analysis demonstrated that mitochondrial volume per proximal tubular cytoplasmic area was

decreased by 22% at 72 hr post cisplatin treatment compared to control sham-injected mouse (percentage area: control, 46.73; cisplatin, 36.76; $p<0.05$; Fig. 3, Panel E). COX enzyme activity, as measured by optical density of reaction product, declined by 40% after cisplatin administration as compared to control animals (mean optical density: control, 54.29; cisplatin, 32.6; $p<0.005$; Fig. 3, Panel F). These results confirm the observation by light microscopy that the decreased COX enzyme activity is attributable to both a decline in mitochondrial density and a loss of mitochondrial enzyme activity. To test whether the mitochondrial damage was greater in the proximal tubule than the distal tubule, we compared these segments 72 hr after cisplatin treatment (Fig. 4). COX enzyme activity is significantly decreased in proximal tubules (Panel B), while it is maintained in distal tubules (Panel D).

Discussion

In this study, we describe how functional and structural impairment of the mitochondria contribute to cisplatin-induced nephrotoxicity in a clinically relevant mouse model (Mukhopadhyay et al. 2012). Cytochrome c oxidase enzyme activity was assessed by light and electron microscopy and protein expression by immunohistochemistry. While COX protein expression was attenuated only in severely damaged tubular epithelium, the decrease in COX enzymatic activity was more significant. Using electron microscopy of proximal tubular epithelial cells, we demonstrate that the decreased COX function is the result of decreased mitochondrial mass as well decreased enzyme activity as measured by reaction product in the mitochondria. Our studies further strengthen previous observations that in mice, the proximal tubular epithelium of the cortex and OSOM are most susceptible to cisplatin treatment.

Several earlier publications have described histopathological findings in mouse models of cisplatin-induced kidney injury. Morphologic changes occurred mainly in the S3 segment of the proximal tubule situated in the outer stripe of the medulla. The characteristic pathologic changes 3 days after cisplatin administration include focal loss of brush border, tubular cell vacuolization, tubular dilation, nuclear pyknosis, and hydropic degeneration, which culminate in tubular cell death (Dobyan et al. 1980; Bulger 1986; Racusen and Solez 1986; Ward and Fauvie 1976). This is consistent with our recent study demonstrating similar pathological alterations on light microscopy level (Mukhopadhyay et al. 2012).

Increased oxidative stress was one of the earliest features associated with the development of cisplatin-induced nephropathy. In the present study, we have provided qualitative data to demonstrate that oxidative and nitrative markers were markedly increased after cisplatin treatment. Substantial evidence has established that oxidative damage is one of the main features of cisplatin nephrotoxicity. Thus, major efforts have been made to test antioxidants that might prevent this type of damage (Matsushima et al. 1998; Davis et al. 2001; Chirino et al. 2004; Chirino et al. 2008; Chirino et al. 2009; Santos et al. 2007). Oxidative stress seems to be the first response to cisplatin; it is followed by the development of proinflammatory response and cell death (Mukhopadhyay, Rajesh, et al. 2010; Mukhopadhyay et al. 2012). These pathological alterations were largely prevented by mitochondrial-targeted antioxidants, which also attenuated the deterioration of the mitochondrial morphology (Mukhopadhyay et al. 2012).

In the present study, we further examined the mitochondrial functional and structural alterations induced by cisplatin in the kidney. While the COX histochemical assay has been applied to other models of renal disease (Holthöfer et al. 1999, nephrotic syndrome; Lebrecht et al. 2004, doxorubicin nephrosis; Tanji et al. 2001, adefovir nephrotoxicity), to our knowledge, this technique has not been applied to explore the mechanisms of mitochondrial injury in a model of cisplatinum nephrotoxicity. In earlier studies using rodent models of cisplatin kidney injury, several other-than-mitochondrial enzymes were measured histochemically, which provided additional mechanistic insight of this disease (Jones et al. 1985; Aggarwal 1993). Our study is the first to apply functional electron microscopy analysis to describe mitochondrial injury in a mouse cisplatin injury model and to perform morphometric analysis quantifiying COX enzyme activity on the ultrastructural level. While enzymatic assays can be done on frozen sections and evaluated by light microscopy, their resolution is insufficient to evaluate individual tubular epithelial cells. Functional electron microscopy analysis clearly indicated that the loss of COX enzyme function in the cortex and OSOM was caused by decreased mitochondrial mass and attenuated enzymatic activity in mitochondria. These findings were strengthened by applying morphometrical assays of electron microscopy images of proximal tubular epithelial cells that demonstrated a significant decrease of COX activity.

Our findings are in good agreement with the emerging mitochondrial damage hypothesis of cisplatin-induced kidney injury observed in cell culture and animal models (Gordon et al. 1986; Brady et al. 1990; Zhang and Lindup 1994; Nowak 2002; Santos et al. 2007; Brooks et al. 2009; Liu et al. 2010; Mukhopadhyay et al. 2012). Kruidering et al. (1997) reported that complexes I to IV of the respiratory chain in the mitochondria were inhibited after 20 min of incubation of proximal tubular cells with cisplatin, resulting in decreased intracellular ATP levels. General antioxidants were not able to prevent the cisplatin-induced decrease in activity of complexes I to IV and cell death in vitro. In contrast, novel mitochondrial-targeted antioxidants (MitoCP and MitoQ) successfully prevented oxidative stress, mitochondrial damage, inflammation, and cell death in cisplatin-induced in vivo

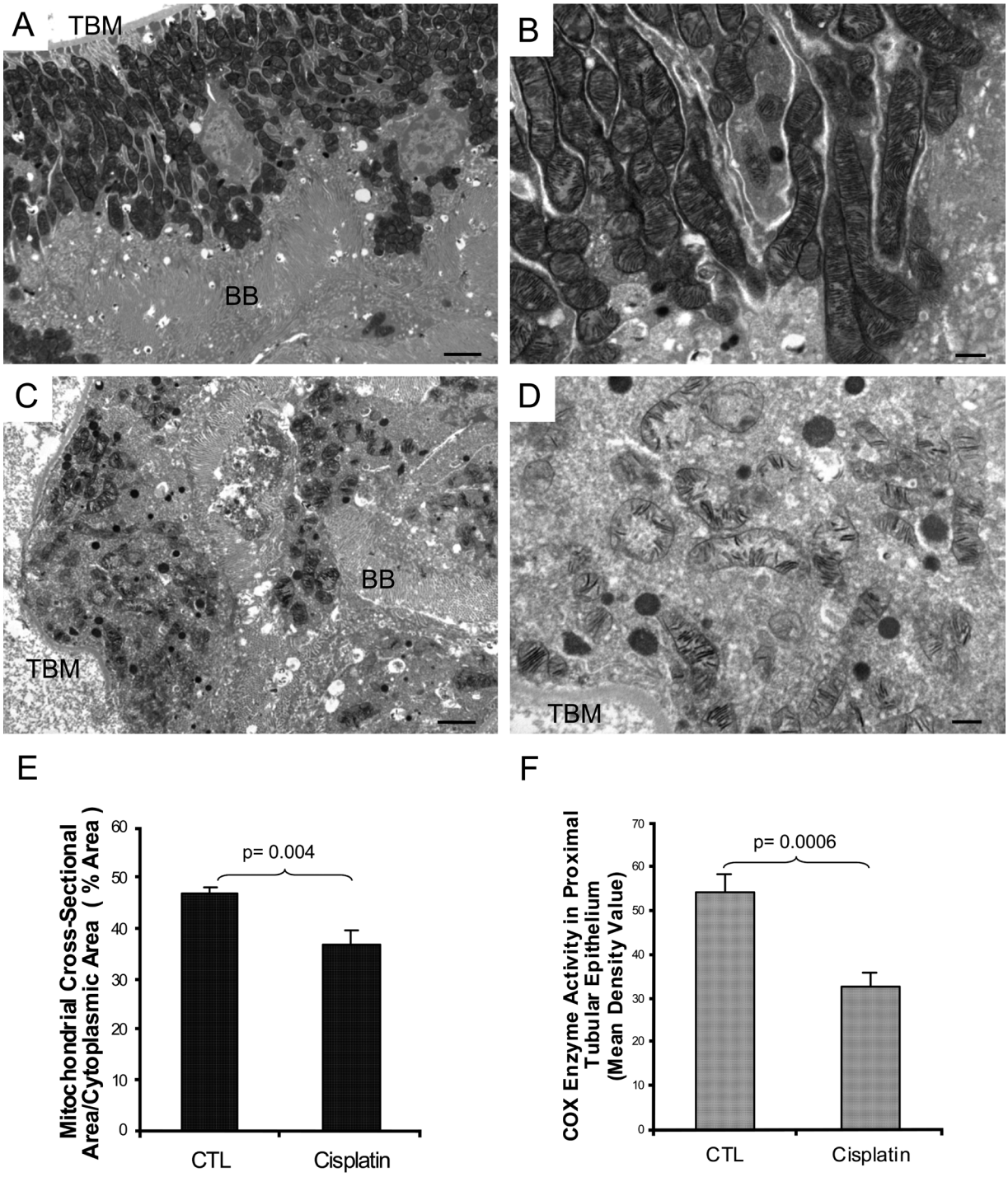

Figure 3. Ultrastructural analysis of mitochondrial cytochrome c oxidase enzyme activity in mouse kidney 72 hr after cisplatin treatment. Functional electron microscopy of the renal cortex in sham-treated control (Panels A and B) shows intact proximal tubular epithelium with preserved mitochondria and intense COX activity in every mitochondria of the cell. In cisplatin-treated kidney (Panels C and D), there is extensive acute injury in the proximal tubule. Disorganized mass of mitochondria, with disrupted cristae and greatly reduced COX activity, is seen. TBM: tubular basement membrane, BB: brush border. Bars in Panels A and C: 2 μm; bars in Panels B and D: 500 nm. Panel E: Morphometric analysis of the mitochondrial volume per proximal tubular cytoplasmic area. Percentage mitochondrial area in tubular epithelium is decreased 72 hr after cisplatin treatment compared to control sham-injected mouse kidney. Data are presented as mean ± SEM. * $p<0.05$, significantly different from sham control. Panel F: Morphometric analysis of COX enzyme activity in mitochondria of the proximal tubular epithelium. COX enzymatic product, measured by mean density value, declined after cisplatin administration compared to control sham-injected mouse kidney. Data are presented as mean ± SEM. ** $p<0.005$, significantly different from sham control.

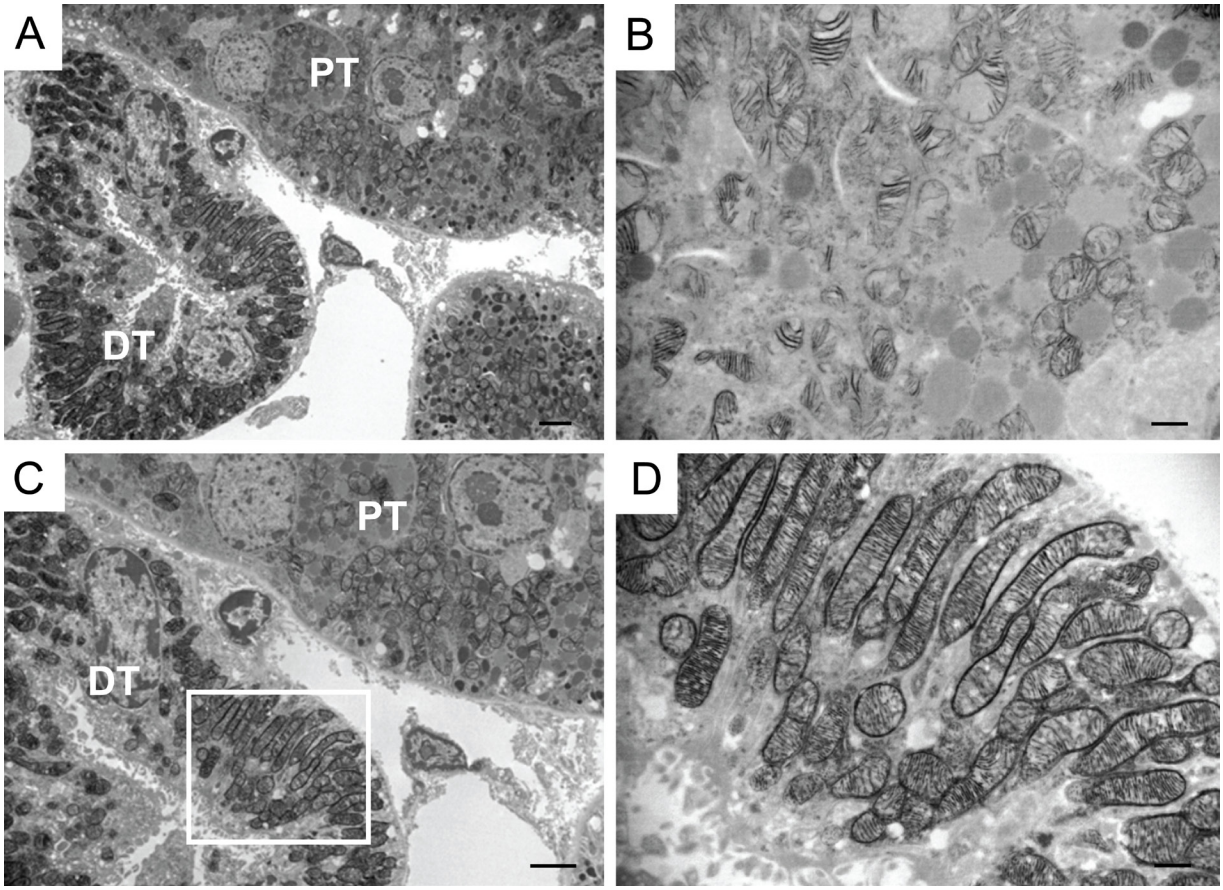

Figure 4. Comparison of different tubular segments in mouse kidneys 72 hr after cisplatin treatment. Ultrastructural analysis of COX enzyme activity in proximal vs distal tubules of a cisplatin-treated mouse (Panels A and C). In proximal tubules, activity is clearly decreased (Panel B), while in distal tubules, COX enzyme activity is maintained (Panel D). DT: distal tubule, PT: proximal tubule. Bars in Panels A and C: 2 µm; bars in Panels B and D: 500 nm.

model of nephropathy (Mukhopadhyay et al. 2012). These antioxidants are SOD mimetics, which can cross the mitochondrial membrane to prevent oxidative injury triggered by cisplatin or other insults.

Immunohistochemical assay for cytochrome c oxidase I did show focal loss of protein expression in denuded proximal tubular epithelium with accompanying dilation of the tubule. However, protein expression in maintained epithelium was not significantly decreased. Cytochrome c oxidase I protein expression was more pronounced in distal tubules, but extensive proximal tubular expression was also seen.

Our functional electron microscopy analysis demonstrates that following cisplatin treatment, distal tubules are less affected compared to proximal tubules and maintain COX enzyme activity. In contrast, proximal tubules are more severely affected and lose most of mitochondrial enzyme activity. It is worth mentioning that pathology of cisplatin nephrotoxicity differs in human and in animals. In humans, kidney tubular damage involves the distal nephron as well (Gonzales-Vitale et al. 1977; Dentino et al. 1978). In our murine model, we find that cisplatin injury is mainly affecting the proximal tubules, which confirms the result of previous findings (Dobyan et al. 1980; Racusen and Solez 1986).

Collectively, our results suggest that cisplatin nephrotoxicity involves important functional alterations in the mitochondria of cortical and OSOM proximal tubules in addition to the structural damage. The assays that we utilized in the current study may also be of help in identifying a role for mitochondrial injury in other renal disorders.

Acknowledgments

We appreciate the critical reading of this manuscript by Dr. Seymour Rosen, Department of Pathology, Beth Israel Deaconess Medical Center, Harvard Medical School, Boston, Massachusetts. S.A.K. is an investigator of the Howard Hughes Medical Institute.

Declaration of Conflicting Interests

The authors declared no potential conflicts of interest with respect to the research, authorship, and/or publication of this article.

Funding

The authors disclosed receipt of the following financial support for the research and/or authorship of this article: This study was supported by the Intramural Program of NIH/NIAAA to PP.

References

Aggarwal SK. 1993. A histochemical approach to the mechanism of action of cisplatin and its analogues. J Histochem Cytochem. 7:1053–1073.

Anderson WA, Bara G, Seligman AM. 1975. The ultrastructural localization of cytochrome oxidase via cytochrome. J Histochem Cytochem. 1:13–20.

Bertoni-Freddari C, Fattoretti P, Casoli T, Di Stefano G, Solazzi M, Gracciotti N, Pompei P. 2001. Mapping of mitochondrial metabolic competence by cytochrome oxidase and succinic dehydrogenase cytochemistry. J Histochem Cytochem. 9:1191–1192.

Brady HR, Kone BC, Stromski ME, Zeidel ML, Giebisch G, Gullans SR. 1990. Mitochondrial injury: an early event in cisplatin toxicity to renal proximal tubules. Am J Physiol. 258(5)(Pt 2):F1181–F1187.

Brooks C, Wei Q, Cho SG, Dong Z. 2009. Regulation of mitochondrial dynamics in acute kidney injury in cell culture and rodent models. J Clin Invest. 119:1275–1285.

Bulger RE. 1986. Renal damage caused by heavy metals. Toxicol Pathol. 1:58–65.

Chirino YI, Hernández-Pando R, Pedraza-Chaverrí J. 2004. Peroxynitrite decomposition catalyst ameliorates renal damage and protein nitration in cisplatin-induced nephrotoxicity in rats. BMC Pharmacol. 4:20.

Chirino YI, Pedraza-Chaverri J. 2009. Role of oxidative and nitrosative stress in cisplatin-induced nephrotoxicity. Exp Toxicol Pathol. 61(3):223–242.

Chirino YI, Trujillo J, Sánchez-González DJ, Martínez-Martínez CM, Cruz C, Bobadilla NA, Pedraza-Chaverri J. 2008. Selective iNOS inhibition reduces renal damage induced by cisplatin. Toxicol Lett. 176(1):48–57.

Davis CA, Nick HS, Agarwal A. 2001. Manganese superoxide dismutase attenuates Cisplatin-induced renal injury: importance of superoxide. J Am Soc Nephrol. 12:2683–2690.

Dentino M, Luft FC, Yum MN, Williams SD, Einhorn LH. 1978. Long term effect of cis-diamminedichloride platinum (CDDP) on renal function and structure in man. Cancer. 4:1274–1281.

Dobyan DC, Levi J, Jacobs C, Kosek J, Weiner MW. 1980. Mechanism of cis-platinum nephrotoxicity: II. Morphologic observations. J Pharmacol Exp Ther. 3:551–556.

Dubowitz V. 1985. Muscle biopsy: a practical approach. 2nd ed. Lavenham, UK: Lavenham Press. p. 21.

Gonzales-Vitale JC, Hayes DM, Cvitkovic E, Sternberg SS. 1977. The renal pathology in clinical trials of cis-platinum (II) diamminedichloride. Cancer. 4:1362–1371.

Gordon JA, Gattone VH 2nd. 1986. Mitochondrial alterations in cisplatin-induced acute renal failure. Am J Physiol. 250(6)(Pt 2):F991–F998.

Hershey SJ, Simon TW, Baste C. 1975. Histochemical localization of cytochrome oxidase in gastric mucosa. J Histochem Cytochem. 4:271–282.

Holthöfer H, Kretzler M, Haltia A, Solin ML, Taanman JW, Schägger H, Kriz W, Kerjaschki D, Schlöndorff D. 1999. Altered gene expression and functions of mitochondria in human nephrotic syndrome. FASEB J. 3:523–532.

Jones TW, Chorpa S, Kaufman JS, Flamenbaum W, Trump BF. 1985. Cis-diamminedichloroplatinum (II)-induced acute renal failure in the rat: enzyme histochemical studies. Toxicol Pathol. 4:296–305.

Kruidering M, Van de Water B, de Heer E, Mulder GJ, Nagelkerke JF. 1997. Cisplatin-induced nephrotoxicity in porcine proximal tubular cells: mitochondrial dysfunction by inhibition of complexes I to IV of the respiratory chain. J Pharmacol Exp Ther. 2:638–649.

Langerak and Dreisbach LP. 2001. Chemotherapy regimens and cancer care. Georgetown, TX: Landes Bioscience.

Lebrecht D, Setzer B, Rohrbach R, Walker UA. 2004. Mitochondrial DNA and its respiratory chain products are defective in doxorubicin nephrosis. Nephrol Dial Transplant. 19:329–336.

Liu L, Yang C, Herzog C, Seth R, Kaushal GP. 2010. Proteasome inhibitors prevent cisplatin-induced mitochondrial release of apoptosis-inducing factor and markedly ameliorate cisplatin nephrotoxicity. Biochem Pharmacol. 2:137–146.

Mahad DJ, Ziabreva I, Campbell G, Lax N, White K, Hanson PS, Lassmann H, Turnbull DM. 2009. Mitochondrial changes within axons in multiple sclerosis. Brain. 5:1161–1174.

Matsushima H, Yonemura K, Ohishi K, Hishida A. 1998. The role of oxygen free radicals in cisplatin-induced acute renal failure in rats. J Lab Clin Med. 131(6):518–526.

Mukhopadhyay P, Horváth B, Kechrid M, Tanchian G, Rajesh M, Naura AS, Boulares AH, Pacher P. 2011. Poly(ADP-ribose) polymerase-1 is a key mediator of cisplatin-induced kidney inflammation and injury. Free Radic Biol Med. 9:1774–1788.

Mukhopadhyay P, Horváth B, Zsengellér Z, Zielonka J, Tanchian G, Holovac E, Kechrid M, Patel V, Stillman IE, Parikh SM, et al. 2012. Mitochondrial-targeted antioxidants represent a promising approach for prevention of cisplatin-induced nephropathy. Free Radic Biol Med. 52(2):497–506.

Mukhopadhyay P, Pan H, Rajesh M, Bátkai S, Patel V, Harvey-White J, Mukhopadhyay B, Haskó G, Gao B, Mackie K, et al. 2010. CB1 cannabinoid receptors promote oxidative/nitrosative stress, inflammation and cell death in a murine nephropathy model. Br J Pharmacol. 3:657–668.

Mukhopadhyay P, Rajesh M, Pan H, Patel V, Mukhopadhyay B, Bátkai S, Gao B, Haskó G, Pacher P. 2010. Cannabinoid-2

receptor limits inflammation, oxidative/nitrosative stress, and cell death in nephropathy. Free Radic Biol Med. 3:457–467.

Nowak G. 2002. Protein kinase C-alpha and ERK1/2 mediate mitochondrial dysfunction, decreases in active Na+ transport, and cisplatin-induced apoptosis in renal cells. J Biol Chem. 45:43377–43388.

Pan H, Mukhopadhyay P, Rajesh M, Patel V, Mukhopadhyay B, Gao B, Haskó G, Pacher P. 2009. Cannabidiol attenuates cisplatin-induced nephrotoxicity by decreasing oxidative/nitrosative stress, inflammation, and cell death. J Pharmacol Exp Ther. 328(3):708–714.

Racusen LC, Solez K. 1986. Nephrotoxic tubular and interstitial lesions: morphology and classification. Toxicol Pathol. 1:45–57.

Ramesh G, Reeves WB. 2002. TNF-alpha mediates chemokine and cytokine expression and renal injury in cisplatin nephrotoxicity. J Clin Invest. 6:835–842.

Ries F, Klastersky J. 1986. Nephrotoxicity induced by cancer chemotherapy with special emphasis on cisplatin toxicity. Am J Kidney Dis. 5:368–379.

Safirstein R, Winston J, Goldstein M, Moel D, Dikman S, Guttenplan J. 1986. Cisplatin nephrotoxicity. Am J Kidney Dis. 5:356–367.

Sahni V, Choudhury D, Ahmed Z. 2009. Chemotherapy-associated renal dysfunction. Nat Rev Nephrol. 8:450–462.

Santos NA, Catão CS, Martins NM, Curti C, Bianchi ML, Santos AC. 2007. Cisplatin-induced nephrotoxicity is associated with oxidative stress, redox state unbalance, impairment of energetic metabolism and apoptosis in rat kidney mitochondria. Arch Toxicol. 7:495–504.

Schrier RW. 2002. Cancer therapy and renal injury. J Clin Invest. 110(6):743–745.

Seligman AM, Karnovsky MJ, Wasserkrug HL, Hanker JS. 1968. Nondroplet ultrastructural demonstration of cytochrome oxidase activity with a polymerizing osmiophilic reagent, diaminobenzidine (DAB). J Cell Biol. 1:1–14.

Tanji N, Tanji K, Kambham N, Markowitz GS, Bell A, D'agati VD. 2001. Adefovir nephrotoxicity: possible role of mitochondrial DNA depletion. Hum Pathol. 7:734–740.

Ward JM, Fauvie KA. 1976. The nephrotoxic effects of cis-diammine-dichloroplatinum (II) (NSC-119875) in male F344 rats. Toxicol Appl Pharmacol. 3:535–547.

Zhang B, Ramesh G, Norbury CC, Reeves WB. 2007. Cisplatin induced nephrotoxicity is mediated by tumor necrosis factor-alpha produced by renal parenchymal cells. Kidney Int. 72:37–44.

Zhang JG, Lindup WE. 1994. Cisplatin nephrotoxicity: decreases in mitochondrial protein sulphydryl concentration and calcium uptake by mitochondria from rat renal cortical slices. Biochem Pharmacol. 7:1127–1135.